UNIQUE HYDROTHERMAL ALTERATION ON MARS: PYRITE-POLYCRYSTALLINE PYRRHOTITE ASSEMBLAGE IN NORTHWEST AFRICA 7034/7533. Jinping Hu[1], Yang Liu[2], P. D. Asimow[1], Chi Ma[1], J. R. Beckett[1] and C. B. Agee[3], [1]Division of Geological and Planetary Sciences, California Institute of Technology, Pasadena CA 91125, email: jinping@caltech.edu, [2]Jet Propulsion Laboratory, California Institute of Technology, Pasadena CA 91109, [3]Institute of Meteoritics, University of New Mexico, Albuquerque, NM 87131

Introduction: NWA 7034 and paired polymict breccia meteorites provide a rich history of surface processes on Mars [1-3]. In particular, multiple thermochronometer systems point to pervasive hydrothermal events in NWA 7034 at 1.3-1.5 Ga [3-4]. It was proposed that secondary pyrite represents the major alteration product in Black Beauty meteorites for that period [5]. Although pyrrhotite ($Fe_{1-x}S$) is a common sulfide in Martian igneous meteorites, previous studies only reported trace pyrrhotite entrained in plagioclase clasts or as isolated spongy veins, separated from pyrite [5]. The occurrence was used to suggest that the pyrrhotite results from local disequilibrium during spatially limited alteration [2, 5]. In this study, we report the discovery of pyrite-pyrrhotite assemblages and isolated large pyrrhotite, plus preliminary crystallographic and chemical characterization of pyrrhotite in NWA 7034/7533. Results indicate that pyrrhotite is more pervasive than previously thought and might be an equilibrium phase of a unique alteration condition.

Methods: Four polished sections of NWA 7034 and 7533 were investigated with scanning electron microscopy (SEM). Composition and structure were determined by energy dispersive X-ray spectroscopy (EDS) and electron backscatter diffraction (EBSD).

Results: *Occurrences of pyrrhotite.* All the pyrrhotite occurs as fine-grained polycrystalline aggregates (Fig. 1 and 2), commonly associated with magnetite. Small aggregates can be ~10 μm in size and entrained in the perthitic feldspar/plagioclase. In contrast, large clasts (100-200 μm) of pyrrhotite were also observed (Fig. 1). These clasts are partially entrained in the breccia matrix and commonly associated with plagioclase and clinopyroxene clasts. Individual pyrrhotite grains are sub-micron to several microns. In Figure 1, EBSD mapping of pyrrhotite shows that adjacent crystals have similar orientation (same IPF color) and might be parts of a larger single crystal. The voids between pyrrhotite crystals are sub-micron and irregularly shaped. The associated silicates are plagioclase and clinopyroxene (Fig. 1b), inferred from the compositions and preliminary EBSP.

One aggregate of pyrrhotite in NWA 7034 is associated with goethite and remnant pyrite (Fig. 2). EBSD mapping shows that the pyrite domains have the same crystallographic orientation (Fig. 2c), suggesting they are remnants of a single crystal. The texture of

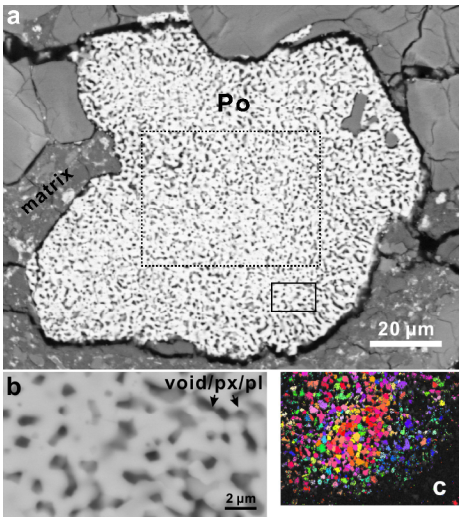

Fig. 1. (a) Back-scattered electron (BSE) image of pyrrhotite (Po) in NWA 7533. (b) High-mag image of the area in the small rectangle in (a) showing dark voids, pyroxene, and plagioclase. (c) EBSD Z-axis inverse pole figure (IPF-Z) for crystals in the large rectangle in (a). Red, green and blue indicate the [001], [010] and [120] zones of pyrrhotite, respectively. Black indicates no diffraction pattern from sample.

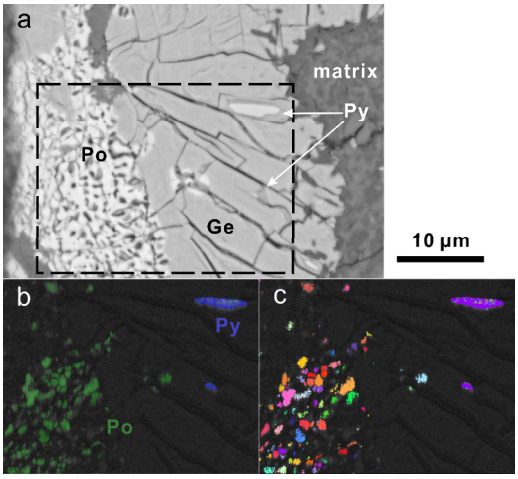

Fig. 2. A pyrrhotite-bearing clast in NWA 7034. (a) BSE image of pyrrhotite (Po)-pyrite (Py)-goethite (Ge) assemblage. (b) EBSD phase map of pyrite (blue) and pyrrhotite (green) in the dash-box in (a). Background is the band contrast. (c) IPF-Z. Red, green and blue indicate the [001], [010] and [120] zones of pyrrhotite, respectively. Purple indicates [110] zone of pyrite.

polycrystalline pyrrhotite is similar to that of Fig. 1. Goethite does not make indexable EBSP and is inferred from the iron/oxygen ratio of EDS analyses.

Pyrrhotite crystal chemistry. Pyrrhotite includes a series of complicated non-stoichiometric compositions and corresponding structures. Deviated from the original NiAs structure (1C, where C is the cell parameter), metal deficiency and vacancy increase lead to structures of Fe_7S_8 (4C), Fe_9S_{10} (5C), $Fe_{10}S_{11}$ (11C), $Fe_{11}S_{12}$ (6C) and other non-stoichiometric structures. The metal deficiency *x* of pyrrhotite $Fe_{1-x}S$ varies from 0.077 to 0.123 in our samples (Fig. 3). Ideally, the measured compositions would adopt a series of structures from 4C to 6C. However, the most common monoclinic 4C structure does not provide the best indices for EBSPs of the pyrrhotite. All the patterns are better indexed by hexagonal structures (NC, N≥5). Because of the small grain size of pyrrhotite, the pattern quality is not sufficient to distinguish among the NC (i.e. 5C, 6C, 11C) structures.

Up to 0.4 wt % of nickel in the pyrrhotite was detected at several localities. More commonly, the Ni content is lower than 0.1 wt %. Contents of other trace elements in pyrrhotite are lower than detection limits of the EDS analysis.

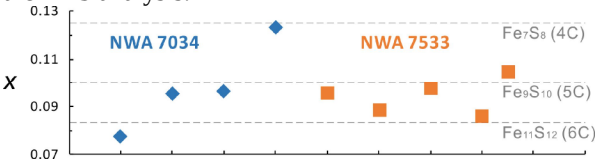

Fig. 3. Metal deficiency x of the $Fe_{1-x}S$ pyrrhotite. The dashed lines show x for stoichiometric compositions.

Discussion: The preferable hexagonal NC structure of pyrrhotite in our samples suggests a relatively low-temperature formation condition [6]. In vacuum, the common 4C-pyrrhotite can co-exist with pyrite up to 290 °C whereas the NC-pyrrhotite is up to 210 °C [6]. At higher temperatures, pyrrhotite is transformed to the so-called NA and MC structures that we do not observe. Hydrothermal alteration, however, is associated with finite sulfur and oxygen fugacities, which affect the phase relations. Increaseing logfS_2 to ~-5 raises the temperature range of co-existing pyrite and NC-pyrrhotite to 470 °C. Presence of possible magnetite with pyrrhotite suggest log$fO2$ of the magnetite-pyrrhotite buffer, ~-22 at 470 °C (Fig. 4). This oxygen fugacity might be significantly different from those indicated by Mn^{4+} materials in NWA 7034/7533 [7], although the pH and Eh of the hydrothermal events are relatively uncertain.

The formation of pyrite-goethite-polycrystalline pyrrhotite is intriguing. Single crystal pyrite and goethite psuedomorphs after pyrite indicate that the assemblage was pyrite-pyrrhotite before late-stage alteration of pyrite to goethite. The phase boundary temperature of the assemblage is ~470 °C (Fig. 4), in agreement with the inferred 400-500 °C crystallization temperature of Ni-rich (4.5 wt%) pyrite [5]. McCubbin et al. used the U-Pb closure temperature in apatite to date a pervasive thermal event at 500-800 °C and 1.5 ± 0.1 Ga [3]. If these features are coeval as reported in [2-5], the temperature difference might result from complex thermal and fugacity histories of the alteration.

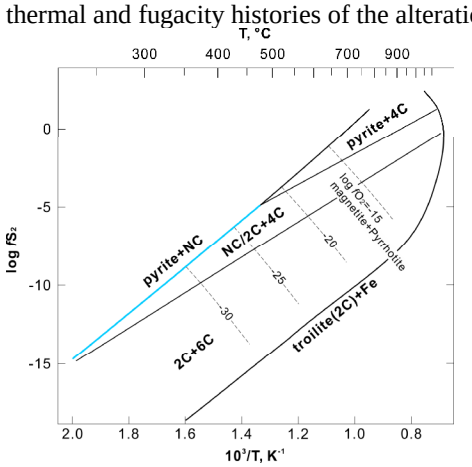

Fig. 4. Sulfur fugacity vs. temperature. Solid lines are phase boundaries between different $Fe_{1-x}S$ structures. Dashed lines are oxygen fugacity of magnetite-pyrrhotite buffer. Blue line denotes the pyrite-pyrrhotite equilibrium boundary. Simplified after [8].

Although the alteration condition can be extracted based on the assumption that pyrrhotite is in equilibrium with pyrite and/or magnetite, it cannot be ruled out that the assemblage represents partial reaction in NWA 7034 and 7533. For instance, previous studies suggest that trace pyrrhotite results from late-stage local alteration of sulfide [2, 5]. If, in fact, the pyrite-pyrrhotite assemblage was formed by pyrite partially replacing the pyrrhotite, as described in some SNC meteorites [5], then pyrite formation is likely part of the proposed pervasive alteration throughout the samples [2-5]. In that case, formation of pyrrhotite would therefore predate the ~1.5 Ga event and record a low temperature (< 400 °C) hydrothermal event that occurred in NWA 7034 before 1.5 Ga.

References:

[1] Agee C. B. et al. (2013) *Science* **339**, 780-785. [2] Hewins et al. (2017) *MAPS* **52**, 89-124. [3] McCubbin et al. (2015) *JGR: Planets* **121**, 2120-2149. [4] Bellucci et al. (2015) *EPSL* **410**, 34-41. [5] Lorand et al. (2015) *MAPS* **50**, 2099-2120. [6] Nakazawa H. and Morimoto N. (1971) *Mat. Res. Bull.* **6**, 345-358. [7] Liu Y. et al. (2017) *LPSC XLVIII* Abstract #1345. [8] Harris D. and Langenhorst F. (2013) *MAPS* **48**, 879-903.